NEAR-END DISTORTION IN OVER-SAMPLED SUBBAND ADAPTIVE IMPLEMENTATION OF AFFINE PROJECTION ALGORITHM

H. Sheikhzadeh, R. L. Brennan, and K. R. L. Whyte

Dspfactory Ltd., 611 Kumpf Drive, Unit 200, Waterloo, Ontario, Canada, N2V 1K8
phone: +1 519 884 9696, fax: +1 519 884 0228,
email: {hsheikh, Robert.brennan, Kevin.whyte}@dspfactory.com, Web: www.dspfactory.com

ABSTRACT

The affine projection algorithm has been employed for echo cancellation using subband adaptive filters implemented with over-sampled filterbanks. We show that the near-end signal may be distorted or partially cancelled if proper regularization is not applied. We attribute these distortions to the nonlinear effects that appear mostly when narrow-band signals are involved in adaptive filtering. Supporting this assumption, it is shown that as the over-sampling rate increases and subband signals become more bandlimited, near-end cancellation also increases. The effect of adaptive filter length and the regularization parameter on near-end distortion is analyzed, leading to the result that near-end distortion can be avoided by proper regularization. As a result, a practical low-cost on-line regularization method is proposed for the affine projection algorithm, effectively eliminating near-end distortion.

1. INTRODUCTION

While Normalized Least Mean Square (NLMS) algorithm is a simple and stable adaptation technique, its convergence is sensitive to the spectral flatness of the reference input and may be very slow for coloured signals. The Recursive Least Squares (RLS) algorithm significantly accelerates the convergence. However, major drawbacks of RLS in practical applications are its high computational requirement and its potential for instability especially in limited precision arithmetic [1].

To reduce computation, the Affine Projection Algorithm (APA) has been introduced as a link between NLMS and RLS [2]. By employing several blocks of input signal rather than one, APA provides convergences faster than NLMS, especially when the reference input of the adaptive filter is highly colored. Furthermore, it requires much fewer computations than the RLS method and is more stable.

In our application, we have implemented APA in the context of Over-Sampled Subband Adaptive Filters (OS-SAFs). OS-SAFs have become a common practical solution [3] because of the well-known advantages of subband processing. Over-sampling greatly simplifies implementation leading to much reduced distortion (aliasing) as compared to critical sampling. In order to reduce group delay while maintaining aliasing at a low level, it is desirable to use a combination of less aggressive analysis and synthesis filters with

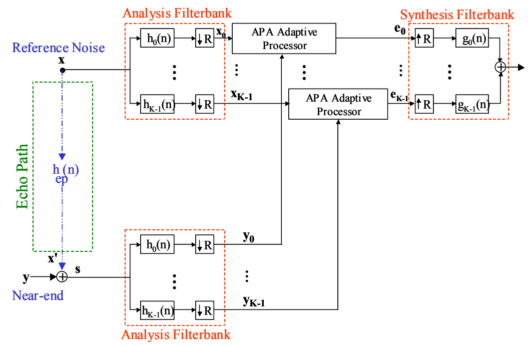

Figure 1: Block diagram of the OS-SAF system.

an over-sampling factor (OS) of two or more [4]. When adaptive filters are used in these highly over-sampled subband structures, the over-sampled inputs to each subband adaptive filter are coloured, leading to slow NLMS convergence. In these situations, the APA is a reasonable alternative adaptation technique.

Fig. 1 shows the block diagram of the OS-SAF system in an echo cancellation set up. The filterbank is a highly over-sampled ($OS \geq 2$), generalized DFT, uniform filterbank [4]. Here, the number of bands is set to $K = 32$ ($K/2$ unique bands due to Hermitian symmetry) and the decimation rate in each subband is R. The over-sampling rate is $OS = K / R$. Each APA adaptive processor contains an FIR filter adapted by the APA.

We show that when the APA is employed to process the colored subband signals of the over-sampled filterbank, near-end (NE) cancellation and distortion occurs. It is well known (for review see [5]) that nonlinear effects occur in NLMS when the reference signal is narrow-band and the adaptation step-size is large. We report similar nonlinear effects in the APA. The effect of APA parameters on the NE distortion is analyzed and an efficient regularization technique is proposed to cope with these distortions.

In the following, Section 2 describes the APA and Section 3 discusses the NE cancellation. A practical regularization technique is proposed in Section 4, and conclusions are provided in Section 5.

2. AFFINE PROJECTION ALGORITHM

The affine projection algorithm can be summarized in three equations [6]:

$$\underline{e}_n = \underline{s}_n - \boldsymbol{X}_n^T \underline{h}_{n-1}$$

$$\underline{\varepsilon}_n = \left[\boldsymbol{X}_n^T \boldsymbol{X}_n + \delta \boldsymbol{I}_N\right]^{-1} \underline{e}_n$$

$$\underline{h}_n = \underline{h}_{n-1} + \mu \boldsymbol{X}_n \underline{\varepsilon}_n$$

where N is the affine order, $\boldsymbol{X}_n = \left[\underline{x}_n, \underline{x}_{n-1}, \cdots, \underline{x}_{n-N+1}\right]$ is the excitation signal matrix ($L \times N$), $\underline{x}_n = \left[x_n, x_{n-1}, \cdots, x_{n-L+1}\right]^T$ is the excitation signal vector, L is the length of the adaptive filter $\underline{h}_n = \left[h_{0,n}, h_{1,n}, \cdots, h_{L-1,n}\right]^T$, and $\boldsymbol{I}_N$ is the $N \times N$ identity matrix. The N-length vectors $\underline{e}_n$, $\underline{\varepsilon}_n$ and s_n are the error (output), the normalized error, and the primary signal vectors respectively. The scalars δ and μ are the regularization and step-size parameters, respectively. The primary signal s_n can be decomposed as

$$\underline{s}_n = \boldsymbol{X}_n^T \underline{h}_{ep} + \underline{y}_n$$

where $\underline{h}_{ep}$ is the echo-path impulse response and $\underline{y}_n$ is the NE disturbance.

3. NEAR-END CANCELLATION IN APA

In various implementations of APA the step-size is often selected close to one, and the regularization parameter is selected to insure the stability of the algorithm. However, as reported in this paper, improper regularization can lead to distortion and cancellation of the primary signal before instability occurs.

3.1 Experiments

The APA was employed in an acoustic echo cancellation (AEC) set up employing the OS-SAF, depicted in Fig. 1. To eliminate other potential sources of NE cancellation, full APA (with no approximation) was applied in each sub-band with fixed regularization of $\delta = 5 \times 10^7$ and $\mu = 1.0$. White noise was employed for the time-domain reference signal. Echo was generated using a typical echo plant at echo return loss of 15 dB. This parameter set and system set up were kept constant through all experiments except where otherwise noted.

The NE signal consisted of a male voice and white noise (at 15 dB SNR), as depicted in bottom half of Fig. 2. To demonstrate NE distortion, the reference signal and the primary signal (consisting of NE disturbance and echo) were applied to the SAF system. Simulations were done with $OS = 4$, adaptive filter length of $L = 24$, and the affine order of $N = 4$. The power of the output signal (in dB) was then subtracted from the power of the NE disturbance in dB. Smoothing this difference with a first-order IIR filter, we arrive at the curve depicted in the top half of Fig. 2. In absence of NE cancellation, this difference should be negative, or at most zero dB when echo is perfectly cancelled. The difference however is positive which indicates that the NE signal is being cancelled. This time-varying cancellation in various subbands results in audible distortion even though

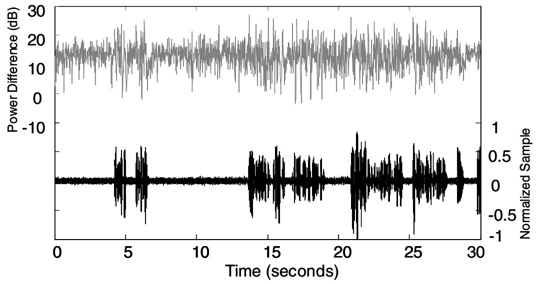

Figure 2: NE speech signal (bottom) and its cancelled portion (top).

Table 1: Power of various signal employed in the experiment

Signal	Output Power (dB)
Primary	-39.46
Reference	-27.47
Echo	-42.46
Near-End	-42.47

Table 2: Output power versus different over-sampling factors for both constant L and scaled L.

OS value for SAF	Scaled L	Output Power (Scaled L) (dB)	Output Power ($L = 128$) (dB)
2	8	-43.02	-50.45
4	16	-51.16	-57.48
8	32	-57.42	-63.47
16	64	-63.81	-66.99
Time-domain APA	128	-39.39	

the system is completely stable. We attribute the NE cancellation to the nonlinear effects of the APA when the reference subband signal becomes narrowband as a result of over-sampling. To validate this assumption, more experiments are carried out.

3.1.1 Effect of Increased Over-sampling on NE cancellation

To analyze the effect of over-sampling, we measured the steady-state performance of the OS-SAF system for echo cancellation using two long white uncorrelated signals as the NE and primary signals. The steady-state input signal powers were measured as depicted in Table 1. The OS value was varied between 2 to 16, and output power of the system was measured. For SAF length, first a constant length of $L = 128$ was employed, and next the length was scaled to maintain the same time-span of the filter for different OS values. 4th order APA (with no approximations) was applied in each sub-band. Table 2 presents the output power for various OS values. For reference, the output power of the time-domain APA system (of order 4) using the same data is also shown. Evidently, the NE cancellation uniformly increases with increased over-sampling since the subband signals become more narrow-band. The trend is similar for both constant and scaled filter length scenarios. However, the time-domain APA exhibits almost no NE cancellation. This experiment confirms that when APA is employed in OS-SAF

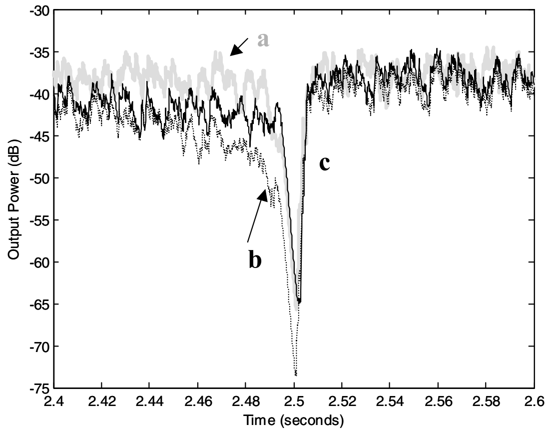

Figure 3: Output power in time for: (a) grey-thick line, $\delta = 5 \times 10^7$, $\mu = 0.7$, $L = 24$, (b) dashed line, $\delta = 5 \times 10^7$, $\mu = 0.7$, $L = 96$, (c) black-thin line, $\delta = 2.5 \times 10^8$, $\mu = 1.575$, $L = 96$.

NE signal cancellation and distortion happens due to subband signal coloration.

3.1.2 Effect of Filter Length on NE cancellation

To better analyse the NE cancellation problem, the following experiment was designed. Two different samples of white noise, both five seconds long, were used for the far-end and NE signals with an echo created using the same echo plant. The APA echo canceller was used for the first half of the simulation. Adaptation was then stopped and the adaptive filter coefficients were saved. Next, a second simulation was run without adaptation using the coefficients of the adaptive filter saved in the first run. The APA parameters were: fixed regularization of $\delta = 5 \times 10^7$, $\mu = 0.7$, $N = 4$ and SAF length of $L = 24$. Curve "a" in Fig. 3 depicts the power, estimated using a first order IIR filter, of the output of the second simulation. It focuses around the time when adaptation was stopped during the first run. It clearly shows that at the point where adaptation was stopped, the power of the output signal is greatly reduced due to the NE cancellation. At this point, the adaptive filter is highly tuned to the NE signal rather than adapting to the echo signal.

For further analysis, consider the noise-amplification factors (NAFs) at time n, denoted by $\tau_{i,n}$, proposed in [6],

$$\tau_{i,n}(\lambda_{i,n}, \delta) = \mu \frac{\sqrt{\lambda_{i,n}}}{\lambda_{i,n} + \delta}$$

where $\lambda_{i,n}$ is the i[th] eigenmode of $\boldsymbol{X}_n^T \boldsymbol{X}_n$. It is shown [6] that the NAFs scale the magnitude of the NE disturbance for each eigenmode of the affine projection in the APA. Fig. 4 shows that increasing δ will result in lower sensitivity to the eigenvalues. We employ the NAFs to gain more insight into the effect of the filter length on NE cancellation. Shown in Fig. 5 (by bars "a") are the (time-averaged) NAFs for the four eigenmodes for the reference signal (in one subband), corresponding to curve "a" in Fig. 3 ($L = 24$). Increasing L to 96 leads to NAFs depicted by bars "b" in Fig. 5. As a result, we expect more NE cancellation (as shown by curve "b" in Fig. 3) due to a dominant eigenmode.

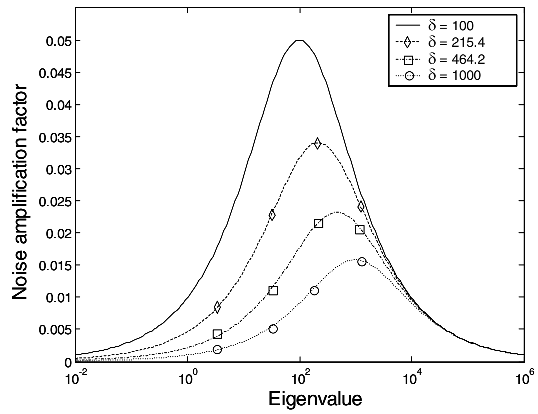

Figure 4: Noise amplification factor versus eigenvalues for various regularization parameters.

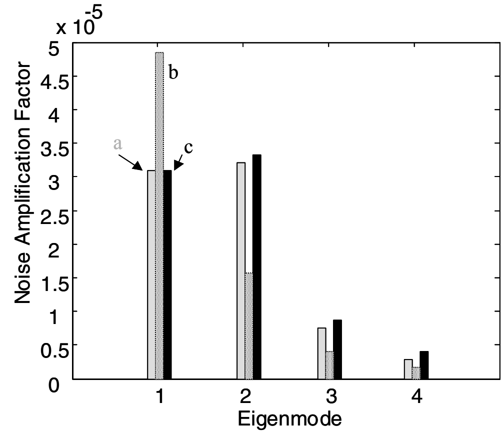

Figure 5: NAFs versus Eigenmodes: for parameter sets (a), (b), and (c) in Fig. 3.

Next we re-adjust the parameters to $\delta = 2.5 \times 10^8$ and $\mu = 1.575$ to obtain NAFs (shown by bars "c" in Fig. 5) for $L = 96$ that are very close to those for $L = 24$. Using these δ and μ values for simulations, we obtain almost identical results with those for $L = 24$, as shown by curve "c" in Fig. 3.

The presented results clearly demonstrate that the filter length affects the NE cancellation by changing the NAFs. The effects of affine order on NE cancellations can be similarly analysed using the NAFs. However, the analysis is more involved and we refrain from discussing it here for brevity.

4. PREVENTING NE DISTORTION

The solution we propose for the NE cancellation is based on proper regularization to suppress the NE disturbance in adaptation. From Fig. 4 it can be seen that an increase in regularization affects the peak of the noise amplification factor (due to the dominant eigenmode) first. This makes online regularization, like those proposed in [7] and [8], highly desirable. Reducing the noise-amplification factors is equivalent to suppressing the NE disturbance in adaptation. Another solution is to decrease step-size. Because step-size and regularization are closely related, increasing regularization suffices.

Here we propose a simplified method based on the online regularization of [8]. In practice, fast versions of APA are employed for real-time implementation. We choose the Gauss-Seidel Fast APA (GSFAP) [9] for its low cost and desirable stability properties. In GSFAP, regularization can serve two purposes: stabilizing the Gauss-Seidel iteration and controlling the NE disturbance. The goal of online regularization is to create a time-varying regularization parameter to serve the two purposes of regularization in a near-optimal manner. We propose the following regularization that comes close to this goal.

$$\delta_n = L \cdot \max\left\{(N-1)\cdot\overline{|x_n|^2}, \overline{|s_n|^2}\right\} \quad (1)$$

where $\overline{|\circ|^2}$ represents the time-averaged power. The first part of Eq. (1), $(N-1)\cdot L\cdot\overline{|x_n|^2}$, addresses the issues of stabilizing the Gauss-Seidel algorithm. It is based on the method proposed in [7] and subsequently modified in [8]

$$\boldsymbol{R}_n = \left[\boldsymbol{X}_n^T\boldsymbol{X}_n + diag\{\underline{\delta}_n\}\right]^{-1} \quad (2)$$

where $\underline{\delta}_n$ is an N-length vector with elements:

$$\delta_{i,n} = \left(\sum_{0\le j<N,\, j\ne i}\left|\underline{x}_{n-i}^T\underline{x}_{n-j}\right|\right) - \left|\underline{x}_{n-i}^T\underline{x}_{n-i}\right| \quad (3)$$

We now approximate (3) to reduce its complexity. For a stationary reference signal, each element of the summation can be approximated (over-estimated) by $L\cdot\sigma_x^2$, where σ_x^2 is the power of the reference signal. This leads to

$$\delta_{i,n} \approx \left(\sum_{0\le j<N,\, j\ne i} L\cdot\sigma_x^2\right) - L\cdot\sigma_x^2 = (N-2)\cdot L\cdot\sigma_x^2 \quad (4)$$

Notice that the regularization is now independent of the row i. We replace $N-2$ by $N-1$ to turn off regularization for NLMS (where $N=1$). Doing so and replacing the reference power with a time-averaged estimate results in

$$\delta_n = (N-1)\cdot L\cdot\overline{|x_n|^2} \quad (5)$$

This is the first part of Eq. (1). While Eq. (5) may give values that are slightly higher than Eq. (3), it is computationally much simpler and our numerous simulations have shown that it ensures stability of the Gauss-Seidel iteration while maintaining a fast convergence rate.

The second part of Eq. (1), $L\cdot\overline{|s_n|^2}$, has its origins in [7], where using the independence assumption and assuming a white reference signal, an optimal regularization parameter is approximated by

$$\delta_{opt,n} \approx \frac{L\cdot\sigma_y^2}{E\left\{\left\|\Delta\underline{h}_n\right\|^2\right\}} \quad (6)$$

However, it is difficult to estimate the expectation of the adaptive filter distance from the ideal solution ($\left\|\Delta\underline{h}_n\right\|^2$) in the denominator, especially when using sub-band adaptive filters. Furthermore, a measurement of the power of the NE disturbance (in the numerator) is simply not available. To avoid these difficulties, it is proposed in [8] to make the following approximation.

$$\delta_n = L\cdot\overline{|s_n|^2} \quad (7)$$

where the power of the NE disturbance is replaced by the estimated power of the entire primary signal. The system distance is also assumed to be approximately one. Eq. (7) is the second part of Eq. (1) that is responsible for controlling the NE disturbance to prevent NE cancellation and distortion We employed the proposed regularization of Eq. (1) in various GSFAP simulations involving realistic situations. The results showed negligible NE cancellation or distortion, while fast convergence was maintained.

5. CONCLUSIONS

It was shown that similar to the NLMS, nonlinear effects exist in the APA and its various implementations. As a result, the NE (primary) signal may be distorted before the system becomes unstable. The issue is of critical importance in OS-SAFs due to the limited bandwidth of the subband signals. The problem can be avoided through a proposed regularization. We are now in the process of providing a mathematical model for the nonlinear effects in APA.

REFERENCES

[1] S. Haykin, *Adaptive Filter Theory*, 3rd ed., Prentice Hall Inc., 1996.

[2] M. Montazeri, and P. Duhamel, “A set of algorithms linking NLMS and block LMS algorithms,” *IEEE Tran. Signal Processing*, vol. 43, no. 2, Feb. 1995.

[3] S. Weiss, “On adaptive filtering in oversampled subbands,” PhD. Thesis, Signal Processing Division, University of Strathclyde, Glasgow, May 1998.

[4] R. Brennan, and T. Schneider, “A flexible filterbank structure for extensive signal manipulation in digital hearing aids,” *Proc. IEEE Int. Symp. Circuits and Systems*, pp. 569-572, 1998.

[5] A. A. Beex and J. R. Zeidler, Steady-state dynamic weight behavior in (N)LMS adaptive filters, in Least-Mean Square Adaptive Filters, S. Haykin and B. Widrow (eds), John Wiley & Sons, NJ, 2003.

[6] S. L. Gay, Fast Projection Algorithms with Application to Voice Excited Echo Cancellers, doctoral dissertation, Rutgers Univ., Piscataway, N.J., Oct. 1994.

[7] V. Myllylä and G. Schmidt, “Pseudo-Optimal Regularization for Affine Projection Algorithms,” *Proc. of ICASSP 2002*, vol. 2, May 2002, pp. 3023-3026.

[8] E. Chau, H. Sheikhzadeh and R. L. Brennan, “Complexity Reduction and Regularization of a Fast Affine Projection Algorithm for Oversampled Subband Adaptive Filters,” *Proc. of the ICASSP 2004*.

[9] F. Albu, J. Kadlec, N. Coleman, and A. Fagan, “The Gaussseidel fast affine projection algorithm,” *Proc. IEEE Workshop on Signal Processing Systems*, pp. 109–114, 2002.